

# Superbunching in cathodoluminescence: a master equation approach

Tatsuro Yuge,<sup>1,\*</sup> Naoki Yamamoto,<sup>2</sup> Takumi Sannomiya,<sup>2</sup> and Keiichirou Akiba<sup>3,†</sup>

<sup>1</sup>*Department of Physics, Shizuoka University, Shizuoka 422-8529, Japan*

<sup>2</sup>*Department of Materials Science and Engineering,  
School of Materials and Chemical Technology, Tokyo Institute of Technology,  
4259 Nagatsuta, Midoriku, Yokohama 226-8503, Japan*

<sup>3</sup>*Takasaki Advanced Radiation Research Institute,  
National Institutes for Quantum Science and Technology,  
1233 Watanuki, Takasaki, Gunma 370-1292, Japan*

We propose a theoretical model of quantum master equation (QME) for cathodoluminescence (CL). The QME describes simultaneous excitation of multiple emitters by an incoming electron and radiative decay of individual emitters. We investigate the normalized second-order correlation function,  $g^{(2)}(\tau)$ , of this model. We derive the exact formula for the zero-time delay correlation,  $g^{(2)}(0)$ , and show that the model successfully describes giant bunching (superbunching) in the CL. We also derive an approximate form of  $g^{(2)}(\tau)$ , which is valid for small excitation rate. Furthermore, we discuss the state of the radiation field of the CL. We reveal that the superbunching results from a mixture of an excited photon state and the vacuum state and that this type of a state is realized in the CL.

## I. INTRODUCTION

In electron microscopy, cathodoluminescence (CL) visualizes optical properties beyond diffraction limit of light. A wide range of materials can be investigated by this approach, for instance, defect/luminescence centers in semiconductors [1–4], quantum-confined structures [5–7], surface plasmon polaritons [8–10], and fluorescent proteins [11–13]. Thus, the electron microscopy-based CL measurement is a powerful tool to analyze various materials on nanoscale.

The optical state of CL itself has not been spot-lighted for a long time though CL had been used in displays with cathode ray tubes for more than a century. By recent introduction of Hanbury Brown-Twiss (HBT) interferometry to CL, the quantum character “antibunching” of the emitted states of CL has been revealed with a deep subwavelength spatial resolution in the measurement of a single nitrogen-vacancy (NV) center in a nanodiamond [14]. Since antibunching is a result from particle nature of a photon, this HBT-CL technique opens a way to measure quantum optical phenomena in nanoscale.

However, the HBT measurement of CL from multiple defect centers has presented strong bunching [15], which has not been observed in photoluminescence (PL) experiment for the same kind of sample. Although there are differences between optical and electron-beam excitations such as absence of  $NV^-$  spectrum in CL [16], this bunching observation raises a question on the origin of the bunching. In addition, the observed bunching in CL is often huge, where the normalized second-order correlation function,  $g^{(2)}(\tau)$ , at time delay  $\tau = 0$  is larger than 2, i.e. superthermal values. This is known as superbunching and a peculiar state of light. A representative

example of the superbunching is spontaneous parametric down-converted light (a squeezed vacuum), which is the quantum light widely used as heralded single photons and entangled photon pairs [17]. Other examples are superradiant coupling of the emitters [18–20], quantum dot-metal nanoparticles [21, 22], and bimodal laser [23–27]. Therefore, it would be interesting and beneficial for the understanding to describe the CL bunching quantum-mechanically.

The bunching in CL has already enabled us to measure luminescent lifetime well below the optical diffraction limit without a pulsed electron beam [28]. This novel time-resolved measurement not only demonstrated the Purcell effect on nanoscale [29, 30] but also quantified excitation and emission efficiencies of optical nanostructures [31, 32]. These practical applications prove that the CL photon correlation has a great potential to access intrinsic nanophotonic properties in a direct manner and offer important insights into nanophotonic devices. Therefore, it is important to clarify how the strong bunching emerges in CL from both basic and applied aspects. The deeper understanding of CL photon correlation should progress nanoscale optical imaging to the next stage.

There were studies on CL photon statistics about half a century ago [33, 34]. These pioneered investigations presented a theoretical description of the photon statistics and an experimental observation of the strong intensity correlation. However, the feature of  $g^{(2)}$  in CL was not focused. In the first report of the superbunching in CL [15], Meuret et al. assumed that plasmons induce a synchronized excitation of multiple emitters and proposed a stochastic model to perform a Monte Carlo simulation on  $g^{(2)}(\tau)$ . On the basis of similar assumptions, CL excitation efficiency was estimated [31], and an analytical model was constructed [35]. Feldman et al. claimed that the bunching in the nanodiamond CL is mediated by the phonon sidebands and explained  $g^{(2)}(\tau)$  using another

\* yuge.tatsuro@shizuoka.ac.jp

† akiba.keiichiro@qst.go.jp

Monte Carlo model [36]. Besides these models, Yanagimoto et al. derived an expression of  $g^{(2)}(\tau)$  using a rate equation for multiple two-level systems [30]. However, the models in all the previous studies are essentially classical, and no quantum model has been proposed that explains the superbunching in CL.

In this study, we introduce a quantum model of multiple emitters in CL. We use a quantum master equation (QME) to describe the dynamics with excitation and decay in CL. After reducing the QME to a master equation for the distribution of number of excited emitters, we obtain the steady state of the distribution. Then, using the steady state, we derive the exact formula for zero-time delay correlation  $g^{(2)}(0)$  and an approximate equation for delay time-dependent correlation  $g^{(2)}(\tau)$ . We show that these results successfully reproduce several features of CL, in particular, the superbunching and the decaying behavior of  $g^{(2)}(\tau)$ . We also deduce the state of the radiation field from a possible sequence of pulses of the field in the CL. From the model calculation and the deduced argument for the radiation field, we shed a light on a universal aspect of the superbunching.

## II. MASTER EQUATION

The system of our interest is composed of  $N$  emitters. Each emitter is modeled by a two-level system (TLS) with transition energy  $\hbar\omega_e$ . The system Hamiltonian is

$$\hat{H} = \sum_{j=1}^N \frac{\hbar\omega_e}{2} \hat{\sigma}_j^z. \quad (1)$$

Here  $\hat{\sigma}_j^z$  is the  $z$ -component of Pauli matrix for the  $j$ th TLS. This is expressed as  $\hat{\sigma}_j^z = |1\rangle_j \langle 1| - |0\rangle_j \langle 0|$  with the lower level state  $|0\rangle_j$  and the upper one  $|1\rangle_j$  of the  $j$ th TLS.

In this study, we consider CL emission with a continuous electron beam. The emitters are continuously excited by the incoming electrons and decay with photon emission. The Lindblad-type quantum master equation (QME) [37–40] is a suitable method for describing dynamics in this situation quantum-mechanically. The QME has the following form:

$$\frac{d}{dt} \hat{\rho}(t) = \mathcal{L} \hat{\rho}(t), \quad (2)$$

where  $\hat{\rho}(t)$  is the state (density matrix) of the system at time  $t$  and the Liouvillian  $\mathcal{L}$  is given by

$$\mathcal{L} \hat{\rho} = \frac{1}{i\hbar} [\hat{H}, \hat{\rho}] + \mathcal{D}_{\text{rad}} \hat{\rho} + \mathcal{D}_{\text{ex}} \hat{\rho}. \quad (3)$$

The first term represents the unitary part of the time evolution with the system Hamiltonian (1). The second and third terms represent the non-unitary parts due to the decay and excitation, respectively, as explained below.

The second term in the Liouvillian (3) describes the radiative decay of the emitters. We here assume that

the dipole moments of the emitters are randomly oriented. In this case, they are independently damped even though the emitters excited by the electron beam are located within a region smaller than the wavelength  $2\pi c/\omega_e$ . Therefore, as in the quantum optical master equation [39–41] under the additional assumption that the reservoir temperature is sufficiently smaller than  $\hbar\omega_e$ , the second term is given in the following Lindblad form:

$$\mathcal{D}_{\text{rad}} \hat{\rho} = \frac{1}{\tau_{\text{rad}}} \sum_{j=1}^N \left( \hat{\sigma}_j^- \hat{\rho} \hat{\sigma}_j^+ - \frac{1}{2} \{ \hat{\sigma}_j^+ \hat{\sigma}_j^-, \hat{\rho} \} \right). \quad (4)$$

Here  $\hat{\sigma}_j^+ = |1\rangle_j \langle 0|$  and  $\hat{\sigma}_j^- = |0\rangle_j \langle 1|$  are the raising and lowering operators of the  $j$ th TLS, respectively. And  $\tau_{\text{rad}}$  is the radiative lifetime of each emitter. We note that we can incorporate the non-radiative decay in the same Lindblad form, in which case we should replace the prefactor  $1/\tau_{\text{rad}}$  with  $1/\tau_{\text{tot}} = 1/\tau_{\text{rad}} + 1/\tau_{\text{non-rad}}$  to include the non-radiative lifetime  $\tau_{\text{non-rad}}$ .

The third term in the Liouvillian (3) describes the excitation of the emitters by an electron beam. In CL, it is considered that an incoming electron excites multiple emitters at a picosecond time scale via several steps of elementary processes [15, 42]. By contrast, according to the results of the HBT experiments of CL, the radiative lifetime  $\tau_{\text{rad}}$  is in the order of nanoseconds. Therefore, the excitation time scale is sufficiently smaller than  $\tau_{\text{rad}}$ , and it is reasonable to consider that the emitters are excited *simultaneously* by a single electron. To incorporate this effect into the Lindblad-type QME (2), we should write the third term as:

$$\mathcal{D}_{\text{ex}} \hat{\rho} = \gamma \left( \hat{\Pi}^+ \hat{\rho} \hat{\Pi}^- - \frac{1}{2} \{ \hat{\Pi}^- \hat{\Pi}^+, \hat{\rho} \} \right), \quad (5)$$

$$\hat{\Pi}^\pm = \bigotimes_{j=1}^N \hat{\sigma}_j^\pm. \quad (6)$$

The Lindblad operator  $\hat{\Pi}^+$  of Eq.(6) raises all the TLSs to the upper levels, which implies the simultaneous excitation of the emitters. The excitation rate  $\gamma$  is the product of the number of incoming electrons per unit time and the probability  $p_{\text{ex}}$  that an electron generates the simultaneous excitation. That is,  $\gamma = (I/e) \times p_{\text{ex}}$ , where  $I$  is an electron-beam current and  $e$  is the elementary charge.

As seen in the next section, the statistics of the number of excited emitters  $\hat{n} = \sum_{j=1}^N \hat{\sigma}_j^+ \hat{\sigma}_j^-$  is useful to investigate the second-order correlation function  $g^{(2)}$ . The statistics is governed by the probability  $P(n, t)$  that the number of excited emitters is  $n$  at time  $t$ . As derived in Appendix A, the QME (2) is reduced to the following master equation for  $P(n, t)$ :

$$\frac{d}{dt} P(0, t) = \frac{1}{\tau_{\text{rad}}} P(1, t) - \gamma P(0, t), \quad (7)$$

$$\frac{d}{dt} P(n, t) = \frac{n+1}{\tau_{\text{rad}}} P(n+1, t) - \frac{n}{\tau_{\text{rad}}} P(n, t), \quad (8)$$

$$\frac{d}{dt} P(N, t) = \gamma P(0, t) - \frac{N}{\tau_{\text{rad}}} P(N, t), \quad (9)$$

where Eq. (8) is for  $1 \leq n \leq N - 1$ .

### III. SECOND-ORDER CORRELATION FUNCTION

#### A. Steady state

In CL with a continuous beam, the system is in the steady state  $\hat{\rho}_{\text{ss}}$ , which is determined by  $\mathcal{L}\hat{\rho}_{\text{ss}} = 0$ . In the following, we write the steady-state average  $\text{Tr}[\hat{\rho}_{\text{ss}} \cdots]$  as  $\langle \cdots \rangle_{\text{ss}}$ .

In the steady state,  $P(n, t)$  also becomes the stationary distribution  $P_{\text{ss}}(n)$ . We obtain the equations that determine  $P_{\text{ss}}(n)$  by setting the left hand sides of Eqs. (7)–(9) to zero. We can exactly solve these equations with the normalization condition  $\sum_{n=0}^N P_{\text{ss}}(n) = 1$  to obtain

$$P_{\text{ss}}(0) = \frac{1}{1 + z_N \tau_{\text{rad}} \gamma}, \quad (10)$$

$$P_{\text{ss}}(n) = \frac{\tau_{\text{rad}} \gamma}{n(1 + z_N \tau_{\text{rad}} \gamma)} \quad (1 \leq n \leq N), \quad (11)$$

where  $z_N = \sum_{m=1}^N (1/m)$ . From  $P_{\text{ss}}(n)$ , we can calculate the steady-state moments of  $\hat{n}$ . The first two are:

$$\langle \hat{n} \rangle_{\text{ss}} = \sum_{n=0}^N n P_{\text{ss}}(n) = \frac{N \tau_{\text{rad}} \gamma}{1 + z_N \tau_{\text{rad}} \gamma}, \quad (12)$$

$$\langle \hat{n}^2 \rangle_{\text{ss}} = \sum_{n=0}^N n^2 P_{\text{ss}}(n) = \frac{N(N+1) \tau_{\text{rad}} \gamma}{2(1 + z_N \tau_{\text{rad}} \gamma)}. \quad (13)$$

We use these moments in calculating  $g^{(2)}$ .

We now investigate the normalized second-order correlation function  $g^{(2)}(\tau)$  in the steady state. This is defined by  $g^{(2)}(\tau) = \langle \mathcal{T} : \hat{I}_{\text{rad}} \hat{I}_{\text{rad}}(\tau) : \rangle_{\text{ss}} / \langle \hat{I}_{\text{rad}} \rangle_{\text{ss}}^2$ , where  $\hat{I}_{\text{rad}}$  is the intensity operator of the radiation field,  $\mathcal{T}$  is the time ordering, and  $::$  is the normal ordering [43]. Thanks to the normalization factor  $\langle \hat{I}_{\text{rad}} \rangle_{\text{ss}}^2$ , collection and detection efficiencies of light and the linear loss of an optical system do not affect the value of  $g^{(2)}$ , and thus defined  $g^{(2)}(\tau)$  describes the second-order correlation that is obtained in the HBT experiments. To proceed further, we again use the assumption that the dipole moments of the emitters are randomly oriented. In this case, the intensity operator reads  $\hat{I}_{\text{rad}} \propto \sum_{j=1}^N \hat{\sigma}_j^+ \hat{\sigma}_j^- = \hat{n}$ . Therefore  $g^{(2)}(\tau)$  is given by

$$g^{(2)}(\tau) = \frac{\sum_{j_1, j_2} \langle \hat{\sigma}_{j_1}^+ \hat{\sigma}_{j_2}^+(\tau) \hat{\sigma}_{j_2}^-(\tau) \hat{\sigma}_{j_1}^- \rangle_{\text{ss}}}{\langle \hat{n} \rangle_{\text{ss}}^2}. \quad (14)$$

Since the steady-state correlation function is symmetric at  $\tau = 0$ , we analyze  $g^{(2)}(\tau)$  for  $\tau \geq 0$  in the following.

#### B. Zero-time delay correlation: superbunching

First, we derive the exact formula for the zero-time delay correlation function  $g^{(2)}(0)$ . At  $\tau = 0$ , we can

rewrite the numerator of Eq. (14) as follows:

$$\begin{aligned} \sum_{j_1, j_2} \langle \hat{\sigma}_{j_1}^+ \hat{\sigma}_{j_2}^+ \hat{\sigma}_{j_2}^- \hat{\sigma}_{j_1}^- \rangle_{\text{ss}} &= \sum_{j_1 \neq j_2} \langle \hat{\sigma}_{j_1}^+ \hat{\sigma}_{j_2}^+ \hat{\sigma}_{j_2}^- \hat{\sigma}_{j_1}^- \rangle_{\text{ss}} \\ &= \langle \hat{n}^2 \rangle_{\text{ss}} - \langle \hat{n} \rangle_{\text{ss}}, \end{aligned} \quad (15)$$

noting that  $\hat{\sigma}_{j_1}^{\pm}$  and  $\hat{\sigma}_{j_2}^{\pm}$  are commutative only if  $j_1 \neq j_2$ . Applying Eqs. (12) and (13), we thus obtain the exact formula for  $g^{(2)}(0)$ :

$$g^{(2)}(0) = \frac{1}{2} \left( z_N + \frac{1}{\tau_{\text{rad}} \gamma} \right) \left( 1 - \frac{1}{N} \right). \quad (16)$$

From this formula, we can easily show that the superbunching,  $g^{(2)}(0) \gg 2$ , is observed for  $\tau_{\text{rad}} \gamma \ll 1$ . Figure 1, which shows  $\gamma$  dependence of  $g^{(2)}(0)$ , illustrates this feature clearly. On the other hand, when  $N = 1$ , we have  $g^{(2)}(0) = 0$  indicating the antibunching. This result implies that excitation of multiple emitters ( $N \geq 2$ ) by a single incoming electron are necessary for the superbunching.

We note that, in the formula (16),  $g^{(2)}(0)$  is proportional to  $1/\gamma$  for  $\tau_{\text{rad}} \gamma \ll 1$ . In Fig. 1, this seems valid for  $\tau_{\text{rad}} \gamma \lesssim 0.1$ . Since the excitation rate  $\gamma$  is proportional to the electron current  $I$  and the excitation efficiency  $p_{\text{ex}}$  as explained below Eq. (6), this means that  $g^{(2)}(0)$  is proportional to  $1/I$  and  $1/p_{\text{ex}}$  for  $\tau_{\text{rad}} \gamma \ll 1$ . Therefore, the formula (16) reproduces the properties of  $g^{(2)}(0)$  discussed in Refs. [30, 31, 35].

We also make a remark on the limitation of this formula. In experiments,  $g^{(2)}(0)$  approaches one for large electron current [15, 31, 35, 36]. However, the theoretical formula (16) of  $g^{(2)}(0)$  approaches  $(1/2)z_N(1 - 1/N) \neq 1$  for large  $\gamma$  (thus for large electron current). This discrepancy could be attributed to a general property of the QME—it is valid for small dissipation and excitation rates [39, 40]. The present model and the formula (16) are applicable for small  $\gamma$ .

#### C. Finite-time delay correlation

Next, we derive an approximate form of  $g^{(2)}(\tau)$  under the assumption of  $N \tau_{\text{rad}} \gamma \ll 1$ . To this end, we apply the quantum regression theorem (QRT) [39, 40] to the correlation function  $\sum_{j_1=1}^N \sum_{j_2=1}^N \langle \hat{\sigma}_{j_1}^+ \hat{\sigma}_{j_2}^+(\tau) \hat{\sigma}_{j_2}^-(\tau) \hat{\sigma}_{j_1}^- \rangle_{\text{ss}} = \sum_{j=1}^N \langle \hat{\sigma}_j^+ \hat{n}(\tau) \hat{\sigma}_j^- \rangle_{\text{ss}}$  in the numerator of Eq. (14). We can derive that this correlation function shows a multiple exponential decay and approaches  $\langle \hat{n} \rangle_{\text{ss}}^2$  [thus  $g^{(2)}(\tau) \rightarrow 1$ ] for  $\tau \rightarrow \infty$ . Furthermore, if we assume  $N \tau_{\text{rad}} \gamma \ll 1$ , we can show that the lowest decay rate is approximately equal to  $\lambda_1 \simeq (1/\tau_{\text{rad}})(1 + N \tau_{\text{rad}} \gamma)$  and the second lowest is  $\lambda_2 \simeq (2/\tau_{\text{rad}})[1 - N(N-1)\tau_{\text{rad}}\gamma/4]$  (see Appendix B for derivation). Therefore, the decaying behavior of  $\sum_{j=1}^N \langle \hat{\sigma}_j^+ \hat{n}(\tau) \hat{\sigma}_j^- \rangle_{\text{ss}}$  is dominated by  $e^{-\lambda_1 \tau}$ .

Combining this decaying behavior with the asymptotic value  $\lim_{\tau \rightarrow \infty} g^{(2)}(\tau) = 1$ , we arrive at an approximate

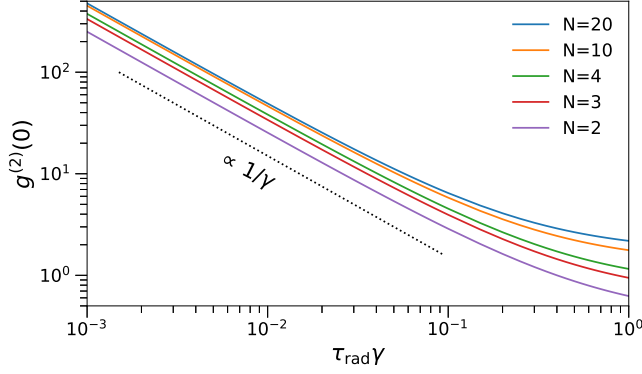


FIG. 1. Zero-time delay correlation  $g^{(2)}(0)$  [Eq. (16)] as a function of the excitation rate  $\gamma$  (normalized by the radiative lifetime  $\tau_{\text{rad}}$ ). The curves from bottom to top correspond to  $N = 2, 3, 4, 10,$  and  $20$ , respectively. The dotted line is an eye guide proportional to  $1/\gamma$ .

expression for  $g^{(2)}(\tau)$ :

$$\begin{aligned} g^{(2)}(\tau) &\simeq [g^{(2)}(0) - 1]e^{-\tau/\tau_{\text{rad}}^{\text{eff}}} + 1 \\ &= C \left(1 - \frac{1}{N}\right) e^{-\tau/\tau_{\text{rad}}^{\text{eff}}} + \left(1 - \frac{1}{N}e^{-\tau/\tau_{\text{rad}}^{\text{eff}}}\right), \end{aligned} \quad (17)$$

In the second line, we used the formula (16) for  $g^{(2)}(0)$ . Here, the effective life time  $\tau_{\text{rad}}^{\text{eff}}$  is given by

$$\frac{1}{\tau_{\text{rad}}^{\text{eff}}} = \frac{1}{\tau_{\text{rad}}} + N\gamma, \quad (18)$$

and the prefactor  $C$  is

$$C = \frac{1}{2} \left( z_N + \frac{1}{\tau_{\text{rad}}\gamma} \right) - 1. \quad (19)$$

We note that our approximate expression (17) has a form similar to that in Ref. [15], which is valid for small  $N$  region. In their expression, the decay time is the bare lifetime  $\tau_{\text{rad}}$  instead of  $\tau_{\text{rad}}^{\text{eff}}$  and the prefactor  $C'$  corresponding to  $C$  in ours reads  $C' = I_0/(I \times P_{\text{el}}^1)$ . In the notation of this paper,  $I_0 = e/\tau_{\text{rad}}$  and the probability of creating electron-hole pairs by an incoming electron  $P_{\text{el}}^1$  should be proportional to  $p_{\text{ex}}$ . Since  $\gamma = (I/e) \times p_{\text{ex}}$  as explained below Eq. (6), we have  $C' \propto 1/(\tau_{\text{rad}}\gamma)$ . In small  $N$  region ( $N\tau_{\text{rad}}\gamma \ll 1$ ), the effective lifetime becomes  $\tau_{\text{rad}}^{\text{eff}} \simeq \tau_{\text{rad}}$  and our prefactor  $C$  of Eq. (19) yields  $C \simeq 1/(2\tau_{\text{rad}}\gamma) \propto 1/(\tau_{\text{rad}}\gamma)$ . Therefore, our result quantum-mechanically validates the form that is derived in Ref. [15].

#### D. Numerical demonstration

To demonstrate the applicability of the approximate expression (17), we compare it with results of numerical simulation. In the simulation, we numerically solve the

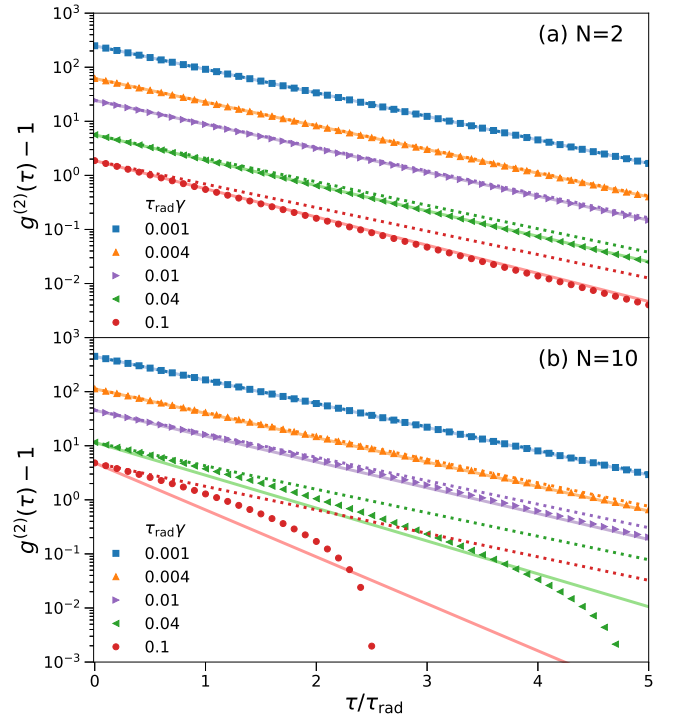


FIG. 2. Normalized second-order correlation function  $g^{(2)}(\tau)$  for (a)  $N = 2$  and (b)  $N = 10$ . Semi-logarithmic plots of  $g^{(2)}(\tau) - 1$  are shown for excitation rates ranging from  $\tau_{\text{rad}}\gamma = 0.001$  to  $0.1$ . The symbols, the solid lines, and the dotted lines represent numerical results, the approximate formula (17), and decay curves proportional to  $e^{-\tau/\tau_{\text{rad}}}$  [Eq. (20)], respectively. For  $\tau_{\text{rad}}\gamma = 0.1$  and  $N = 10$  [filled circles in (b)], data points for  $\tau/\tau_{\text{rad}} \gtrsim 2.5$  are not shown because  $g^{(2)}(\tau) - 1$  is extremely small ( $g^{(2)}(\tau) \approx 1$ ) in this region.

eigenvalue problem of  $\mathcal{L}$  to obtain the steady state  $\hat{\rho}_{\text{ss}}$  as the right eigenvector corresponding to its zero eigenvalue. Then, we use the QRT to compute  $g^{(2)}(\tau)$ . We plot the results for  $N = 2$  and  $N = 10$  in Fig. 2. We also plot Eq. (17) (solid lines) and its variant where  $\tau_{\text{rad}}^{\text{eff}}$  is replaced with  $\tau_{\text{rad}}$  (dotted lines):

$$g^{(2)}(\tau) \simeq C \left(1 - \frac{1}{N}\right) e^{-\tau/\tau_{\text{rad}}} + \left(1 - \frac{1}{N}e^{-\tau/\tau_{\text{rad}}}\right). \quad (20)$$

In the case of  $N = 2$ , Fig. 2(a) shows that the approximate expression (17) describes the numerical data well. In comparison, although Eq. (20) deviates from the numerical results for  $\tau_{\text{rad}}\gamma \geq 0.04$  ( $N\tau_{\text{rad}}\gamma \geq 0.08$ ), it also describes the numerical data well for smaller  $\tau_{\text{rad}}\gamma$  because  $\tau_{\text{rad}}^{\text{eff}} \simeq \tau_{\text{rad}}$  in this regime.

In the case of  $N = 10$ , Fig. 2(b) shows that Eq. (17) well approximates the numerical data for  $\tau_{\text{rad}}\gamma \leq 0.004$  ( $N\tau_{\text{rad}}\gamma \leq 0.04$ ). As  $\tau_{\text{rad}}\gamma$  becomes larger, we observe clearer deviations between the numerical results and Eq. (17) as well as Eq. (20).

From the results of  $N = 2$  and  $N = 10$ , we conclude that the approximation by Eq. (17) is valid for small



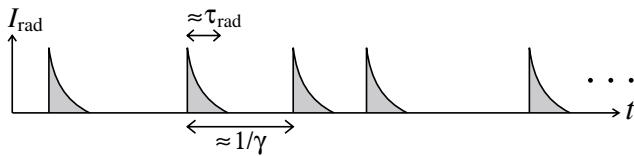


FIG. 3. A sequence of random pulses of radiation intensity.

$N\tau_{\text{rad}}\gamma$ . We also note that the cruder approximation by Eq. (20) is valid if  $N\tau_{\text{rad}}\gamma$  is sufficiently small, and the decay rate of  $g^{(2)}(\tau)$  can be used for estimation of the lifetime  $\tau_{\text{rad}}$  of the emitters. In experiments, one should carefully choose electron-beam current  $I$  in order to obtain the lifetime  $\tau_{\text{rad}}$  from the HBT measurement.

#### IV. STATE OF RADIATION FIELD

In the previous section, our analysis on  $g^{(2)}$  of the radiation field is based on the steady state  $\hat{\rho}_{\text{ss}}$  of the emitters. Understanding the state of radiation field itself is also an interesting problem. In this section, we give a heuristic argument on this problem under the assumption of  $\tau_{\text{rad}}\gamma \ll 1$ .

We first revisit the process of the radiation in CL. Even though an electron beam irradiates a sample continuously, each electron in the beam exists discretely. An incoming electron excites multiple (say,  $N$ ) emitters and the emitters decay with radiating photons. The radiation generated in this process is considered to have a time profile of the intensity  $I_{\text{rad}}(t)$  that is composed of a sequence of random pulses, as schematically depicted in Fig. 3. In each pulse, the excited emitters radiate photons within the duration of the emission process; the duration is random due to the spontaneous emission process of the emitters, and the mean duration is roughly equal to the lifetime  $\tau_{\text{rad}}$ . The instance at which a single pulse starts is also random reflecting the randomness of the incoming electrons, and the mean time between successive pulses is equal to  $1/\gamma$ , where  $\gamma$  is the excitation rate.

From the above argument, we can classify total time of photodetection into pulse-existing regions and zero-intensity regions, and we estimate the ratio  $q$  of the former regions to the total as  $q \approx \tau_{\text{rad}}\gamma (\ll 1)$ . In the former regions, the radiation field is in a certain photonic state  $\hat{\rho}_N^{\text{rad}}$  whose average photon number is around  $N$ . In the latter, it is in the vacuum state  $\hat{\rho}_{\text{vac}}^{\text{rad}} = |\text{vac}\rangle\langle\text{vac}|$ . Therefore, we can consider the steady state of the radiation field in CL as the average of  $\hat{\rho}_N^{\text{rad}}$  and  $\hat{\rho}_{\text{vac}}^{\text{rad}}$ :

$$\hat{\rho}_{\text{avg}}^{\text{rad}} = q\hat{\rho}_N^{\text{rad}} + (1 - q)\hat{\rho}_{\text{vac}}^{\text{rad}}. \quad (21)$$

We can illustrate that this steady state describes the superbunching. Here, we use the single-mode approximation of the radiation field and  $\hat{\rho}_N^{\text{rad}} \approx |N\rangle\langle N|$ , where  $|N\rangle$  is the  $N$ -photon state of the single mode. Then, the zero-time delay correlation function of the radiation field

yields

$$\begin{aligned} g^{(2)}(0) &= \frac{\text{Tr}[\hat{\rho}_{\text{avg}}^{\text{rad}} \hat{a}^\dagger \hat{a}^\dagger \hat{a} \hat{a}]}{\text{Tr}[\hat{\rho}_{\text{avg}}^{\text{rad}} \hat{a}^\dagger \hat{a}]^2} \\ &= \frac{1}{q} \times \frac{\text{Tr}[\hat{\rho}_N^{\text{rad}} \hat{a}^\dagger \hat{a}^\dagger \hat{a} \hat{a}]}{\text{Tr}[\hat{\rho}_N^{\text{rad}} \hat{a}^\dagger \hat{a}]^2} = \frac{1}{q} \left(1 - \frac{1}{N}\right), \end{aligned} \quad (22)$$

where  $\hat{a}^\dagger$  and  $\hat{a}$  are the creation and destruction operators of the mode, respectively. This result with  $q \approx \tau_{\text{rad}}\gamma$  is approximately equal to the exact formula (16) under the condition of  $z_N\tau_{\text{rad}}\gamma \ll 1$ , so that the state in Eq. (21) gives rise to the superbunching,  $g^{(2)}(0) \gg 1$  for  $N \geq 2$ .

For different systems, similar arguments are given in Refs. [44, 45]: a classical (incoherent) mixture of high- and low-intensity states with a large weight on the lower as in Eq. (21) leads to an enhancement of  $g^{(2)}(0)$ . We note that a quantum superposition state  $\sqrt{q}|\text{rad}_N\rangle + \sqrt{1-q}|\text{vac}\rangle$  with some pure photonic state  $|\text{rad}_N\rangle$  such as  $|N\rangle$  also leads to a similar enhancement [45] and, only from  $g^{(2)}(0)$ , it is impossible to distinguish whether the radiation state is a classical or quantum mixture. In our model of CL, however, it should be a classical one because the steady state of the emitters is diagonal in the standard basis.

We also note that this argument can explain the difference between CL and PL photon statistics: the superbunching is observed in the CL whereas  $g_{\text{PL}}^{(2)}(0) \simeq 1$  for the PL of the same sample [15]. The typical coherence time of the continuous wave laser beam used for PL is longer than the radiation lifetime, so that the radiation in PL is not pulsed (as in Fig. 3) but continuous. Therefore, the state of the PL radiation field is simply  $\hat{\rho}_N^{\text{rad}}$  (not mixed with the vacuum state).

#### V. DISCUSSION AND SUMMARY

In this study, we have constructed a QME model that captures essential aspects of CL: simultaneous excitation and individual decay of emitters. We have derived the exact formula for the zero-time delay correlation  $g^{(2)}(0)$ , which successfully describes the superbunching. We have also derived an approximate form for the finite-time delay correlation  $g^{(2)}(\tau)$ , which shows that the radiative lifetime  $\tau_{\text{rad}}$  can be extracted from its  $\tau$  dependence for small  $N\tau_{\text{rad}}\gamma$ .

We have assumed that the emitters have the same transition energy  $\hbar\omega_e$  and radiative lifetime  $\tau_{\text{rad}}$ . Also, they have randomly-oriented dipole moments and are located within a region smaller than the wavelength  $2\pi c/\omega_e$ . Our main conclusion on the superbunching in the CL is not affected by relaxing some of these assumptions.

In the model, the simultaneous excitation of multiple emitters by an incoming electron is phenomenologically incorporated in Eq. (5). It is an important future work to derive this excitation effect by a quantum mechanical analysis on elementary processes in CL. Another implication of this phenomenological incorporation is that

the superbunching is not specific to CL experiments; we can observe superbunching if the simultaneous excitation of multiple emitters is possible. Indeed, giant photon bunching can be observed in other systems that have cooperative emission [20, 46, 47]. In these systems, we can interpret that excitations via dark states play the role of the simultaneous excitation of multiple emitters. In a similar manner, we can explain another example of giant bunching in a system composed of a quantum dot and a metal nanoparticle [21]: in this system, since the transition rate is suppressed by the Fano destructive interference, multiple photons can be efficiently excited through the dark state. This plays the role of (nearly) simultaneous multiple excitation.

We have also discussed a possible state of radiation field in the CL. Through a heuristic argument, we have proposed the state in Eq. (21) and confirmed that it is consistent with the QME analysis and well describes superbunching. This result implies that we may observe superbunching with mechanisms other than the simultaneous excitation of multiple emitters. Indeed, in Ref. [48], an enhancement of  $g^{(2)}(0)$  is discussed in a train of pulses with a regular interval. Our argument, schematically depicted in Fig. 3, shows that the same enhancement is observed in random pulses and that the state of the radiation field in CL should be similar to that of the randomly modulated optical beam. Also, Ref. [44] discusses superbunching with states similar to Eq. (21) and shows that a bimodal microcavity laser with an emitter achieves such a state as its steady state. Indeed, superbunching is reported in bimodal microlaser systems [23–27].

In other words, a potent way to observe superbunching is generating a mixture of photonic states as in Eq. (21), and there are several systems and methods which can generate this type of states. The present study by the master equation reveals that the simultaneous excitation of multiple emitters in CL is one of them and gives quantum insight into CL photon statistics. Since the time correlation measurement of CL has given new functionalities to nanoscale optical imaging, the obtained results imply a potential of CL to reveal and even utilize quantum nature of light-matter interaction in nanoscale.

## ACKNOWLEDGMENTS

We acknowledge Kenji Kamide and Sotatsu Yanagimoto for helpful comments. One of the authors (K. A.) is grateful to Takeshi Ohshima for his kind support of the research. This work was supported by Research Foundation for Opto-Science and Technology and JSPS KAKENHI Grant Numbers JP18K03454, JP21K18195, JP22H01963, and JP22H05032.

## Appendix A: Master equation for $P(n, t)$

In this Appendix, we derive the master equation for the number of excited emitters [Eqs. (7)–(9)]. For this purpose, we introduce some notation. We denote each of the standard basis states as  $|s\rangle = \otimes_{j=1}^N |s_j\rangle_j$  with  $s = \sum_{j=1}^N 2^{j-1} s_j$ . Then, the standard basis is represented as  $\{|s\rangle \mid s = 0, 1, 2, \dots, 2^N - 1\}$ . We write the diagonal elements of the system state  $\hat{\rho}(t)$  as  $\rho(s, t) = \langle s | \hat{\rho}(t) | s \rangle$ . In addition, we define  $|s^{j+}\rangle = \hat{\sigma}_j^+ |s\rangle$ , which is also one of the standard basis states if  $s_j = 0$ .

From the QME (2), we can show  $\langle s | \{d\hat{\rho}(t)/dt\} | s \rangle = \langle s | \mathcal{L}\hat{\rho}(t) | s \rangle$  yields

$$\frac{\partial}{\partial t} \rho(0, t) = \frac{1}{\tau_{\text{rad}}} \sum_{j=1}^N \rho(0^{j+}, t) - \gamma \rho(0, t), \quad (\text{A1})$$

$$\frac{\partial}{\partial t} \rho(s, t) = \frac{1}{\tau_{\text{rad}}} \sum_{j=1}^N \left[ \rho(s^{j+}, t) \delta_{s_j, 0} - \rho(s, t) \delta_{s_j, 1} \right], \quad (\text{A2})$$

$$\frac{\partial}{\partial t} \rho(2^N - 1, t) = -\frac{N}{\tau_{\text{rad}}} \rho(2^N - 1, t) + \gamma \rho(0, t), \quad (\text{A3})$$

where Eq. (A2) is for  $1 \leq s \leq 2^N - 2$ . We note that Eqs. (A1)–(A3) form a closed set of equations for the diagonal elements.

To transform Eqs. (A1)–(A3) to the master equation for  $P(n, t)$ , we note the connection between  $P(n, t)$  and  $\rho(s, t)$ :

$$P(n, t) = \sum_{s=0}^{2^N-1} \rho(s, t) \delta_{n_s, n}, \quad (\text{A4})$$

where

$$n_s = \sum_{j=1}^N s_j = \sum_{j=1}^N \delta_{s_j, 1} \quad (\text{A5})$$

is the number of excited emitters in the state  $|s\rangle$ . Differentiating Eq. (A4) with respect to  $t$  and using Eqs. (A1)–(A3), we obtain the master equation for  $P(n, t)$  [Eqs. (7)–(9)].

## Appendix B: A perturbative analysis of decay rates

In this Appendix, we evaluate the decay rates of  $\sum_{j=1}^N \langle \hat{\sigma}_j^+ \hat{n}(\tau) \hat{\sigma}_j^- \rangle_{\text{ss}}$ . To this end, it is sufficient to investigate each term  $\langle \hat{\sigma}_j^+ \hat{n}(\tau) \hat{\sigma}_j^- \rangle_{\text{ss}}$  in the sum. In the estimation, we use the QRT and a perturbative analysis under the assumption of  $\tau_{\text{rad}} \gamma \ll 1$ .

We first note that  $\hat{n} = \sum_{n=0}^N n \hat{P}_n$ , where  $\hat{P}_n$  is the projection operator onto the subspace of states with  $n$  excited emitters. This leads to  $\langle \hat{\sigma}_j^+ \hat{n}(\tau) \hat{\sigma}_j^- \rangle_{\text{ss}} = \sum_n n \langle \hat{\sigma}_j^+ \hat{P}_n(\tau) \hat{\sigma}_j^- \rangle_{\text{ss}}$ , so that it is reasonable to investigate the decaying behavior of  $\langle \hat{\sigma}_j^+ \hat{P}_n(\tau) \hat{\sigma}_j^- \rangle_{\text{ss}}$ .

According to the QRT,  $\langle \hat{\sigma}_j^+ \hat{P}_n(\tau) \hat{\sigma}_j^- \rangle$  obeys the differential equation whose form is the same as that of  $\langle \hat{P}_n(\tau) \rangle = P(n, \tau)$ . The latter is the master equation for  $P(n, t)$  [Eqs. (7)–(9)], which is expressed as  $d\mathbf{P}(t)/dt = -\Gamma\mathbf{P}(t)$  with  $\mathbf{P}(t) \equiv (P(0, t), P(1, t), \dots, P(N, t))^T$  ( $\Gamma$  stands for transpose) and an  $(N+1) \times (N+1)$  matrix  $\Gamma$ :

$$\Gamma = \begin{pmatrix} \gamma & -1/\tau_{\text{rad}} & & & & \\ & 1/\tau_{\text{rad}} & -2/\tau_{\text{rad}} & & & \\ & & 2/\tau_{\text{rad}} & \ddots & & \\ & & & \ddots & -N/\tau_{\text{rad}} & \\ -\gamma & & & & & N/\tau_{\text{rad}} \end{pmatrix}. \quad (\text{B1})$$

Therefore, by using the QRT, we obtain the differential equation  $d\mathbf{Q}_j(\tau)/d\tau = -\Gamma\mathbf{Q}_j(\tau)$  for  $\mathbf{Q}_j(\tau) \equiv (\langle \hat{\sigma}_j^+ \hat{P}_0(\tau) \hat{\sigma}_j^- \rangle_{\text{ss}}, \langle \hat{\sigma}_j^+ \hat{P}_1(\tau) \hat{\sigma}_j^- \rangle_{\text{ss}}, \dots, \langle \hat{\sigma}_j^+ \hat{P}_N(\tau) \hat{\sigma}_j^- \rangle_{\text{ss}})^T$ . Moreover, using the eigenvalues  $\lambda_n$  and its corresponding left and right eigenvectors,  $\boldsymbol{\ell}_n$  and  $\mathbf{r}_n$ , of the non-Hermitian matrix  $\Gamma$ , we can show

$$\mathbf{Q}_j(\tau) = \sum_{n=0}^N [\boldsymbol{\ell}_n \cdot \mathbf{Q}_j(0)] \mathbf{r}_n e^{-\lambda_n \tau}. \quad (\text{B2})$$

This implies that  $\langle \hat{\sigma}_j^+ \hat{n}(\tau) \hat{\sigma}_j^- \rangle_{\text{ss}}$  exhibits a multiple exponential decay with the rates  $\lambda_n$  ( $n = 1, 2, \dots, N$ ).

Note that, as shown in Eqs. (10) and (11),  $\Gamma$  has a zero eigenvalue  $\lambda_0 = 0$  and the corresponding right eigenvector is  $\mathbf{r}_0 = \mathbf{P}_{\text{ss}} \equiv (P_{\text{ss}}(0), P_{\text{ss}}(1), \dots, P_{\text{ss}}(N))^T$ . And it is straightforward to show that the corresponding left eigenvector is  $\boldsymbol{\ell}_0 = (1, 1, \dots, 1)^T$ . From this result, we can show that the asymptotic value of  $\mathbf{Q}_j(\tau)$  is  $\lim_{\tau \rightarrow \infty} \mathbf{Q}_j(\tau) = [\boldsymbol{\ell}_0 \cdot \mathbf{Q}_j(0)] \mathbf{r}_0 = \langle \hat{\sigma}_j^+ \hat{\sigma}_j^- \rangle_{\text{ss}} \mathbf{P}_{\text{ss}}$ , where we used  $\sum_n \hat{P}_n = 1$ . Therefore, we obtain  $\lim_{\tau \rightarrow \infty} \sum_j \langle \hat{\sigma}_j^+ \hat{n}(\tau) \hat{\sigma}_j^- \rangle_{\text{ss}} = \sum_j \sum_n n \langle \hat{\sigma}_j^+ \hat{\sigma}_j^- \rangle_{\text{ss}} P_{\text{ss}}(n) = \langle \hat{n} \rangle_{\text{ss}}^2$ , which leads to  $\lim_{\tau \rightarrow \infty} g^{(2)}(\tau) = 1$ .

Now we perturbatively estimate the eigenvalues by assuming  $\tau_{\text{rad}}\gamma \ll 1$ . For this purpose, we decompose  $\Gamma$  as  $\Gamma = \Gamma^0 + \gamma\Gamma^1$ . The unperturbed part  $\Gamma^0$  is the matrix where  $\gamma$  in Eq. (B1) is replaced with zero. The perturbation matrix  $\Gamma^1$  has only two non-zero elements:  $\Gamma_{0,0}^1 = 1$  and  $\Gamma_{N,0}^1 = -1$ .

Since  $\Gamma^0$  is an upper triangular matrix, its eigenvalues (the zeroth order eigenvalues  $\lambda_n^0$ ) are the diagonal elements of  $\Gamma^0$ , that is,  $\lambda_n^0 = n/\tau_{\text{rad}}$  ( $0 \leq n \leq N$ ). The corresponding (zeroth order) left and right eigenvectors,  $\boldsymbol{\ell}_n^0$  and  $\mathbf{r}_n^0$ , are determined by

$$(\Gamma^0)^T \boldsymbol{\ell}_n^0 = \lambda_n^0 \boldsymbol{\ell}_n^0, \quad (\text{B3})$$

$$\Gamma^0 \mathbf{r}_n^0 = \lambda_n^0 \mathbf{r}_n^0, \quad (\text{B4})$$

with the normalization  $\boldsymbol{\ell}_n^0 \cdot \mathbf{r}_n^0 = 1$ . After some algebraic calculation, we obtain

$$\boldsymbol{\ell}_n^0 = \left( \underbrace{0, \dots, 0}_n, 1, \binom{n+1}{1}, \binom{n+2}{2}, \dots, \binom{N}{N-n} \right)^T, \quad (\text{B5})$$

$$\mathbf{r}_n^0 = \left( (-1)^n \binom{n}{n}, (-1)^{n-1} \binom{n}{n-1}, \dots, (-1) \binom{n}{1}, 1, \underbrace{0, \dots, 0}_{N-n} \right)^T, \quad (\text{B6})$$

where  $\binom{m}{k} = m!/[k!(m-k)!]$  is a binomial coefficient.

The perturbative analysis for a non-Hermitian matrix is almost the same as that for Hermitian cases in quantum mechanics [49]—the first order correction to the eigenvalue is

$$\begin{aligned} \lambda_n^1 &= \gamma \boldsymbol{\ell}_n^0 \cdot \Gamma^1 \mathbf{r}_n^0 \\ &= \begin{cases} 0 & (n=0) \\ \gamma (-1)^{n+1} \binom{N}{N-n} & (1 \leq n \leq N). \end{cases} \end{aligned} \quad (\text{B7})$$

Therefore, in the first order of  $\tau_{\text{rad}}\gamma$ , we obtain an approximate form of the eigenvalues of  $\Gamma$  (except for the zero eigenvalue  $\lambda_0 = 0$ ):

$$\lambda_n \simeq \frac{n}{\tau_{\text{rad}}} \left[ 1 + \frac{(-1)^{n+1} \tau_{\text{rad}} \gamma}{n} \binom{N}{N-n} \right] \quad (1 \leq n \leq N). \quad (\text{B8})$$

We thus estimate the decay rates  $\{\lambda_n\}_{n=1}^N$  of  $\langle \hat{\sigma}_j^+ \hat{n}(\tau) \hat{\sigma}_j^- \rangle_{\text{ss}}$ . In particular, when  $N\tau_{\text{rad}}\gamma \ll 1$ , the lowest rate is  $\lambda_1 \simeq (1/\tau_{\text{rad}})(1 + N\tau_{\text{rad}}\gamma)$  and the second lowest is  $\lambda_2 \simeq (2/\tau_{\text{rad}})[1 - N(N-1)\tau_{\text{rad}}\gamma/4]$ .

- 
- [1] M. A. S. Kalceff and M. R. Phillips, Cathodoluminescence microcharacterization of the defect structure of quartz, *Phys. Rev. B* **52**, 3122 (1995).  
[2] T. Mitsui, N. Yamamoto, T. Tadokoro, and S.-i. Ohta, Cathodoluminescence image of defects and luminescence centers in ZnS/GaAs(100), *J. Appl. Phys.* **80**, 6972 (1996).  
[3] A. Tararan, S. di Sabatino, M. Gatti, T. Taniguchi, K. Watanabe, L. Reining, L. H. G. Tizei, M. Kociak, and A. Zobelli, Optical gap and optically active intragap defects in cubic BN, *Phys. Rev. B* **98**, 094106 (2018).  
[4] T. Bidaud, J. Moseley, M. Amarasinghe, M. Al-Jassim,

- W. K. Metzger, and S. Collin, Imaging CdCl<sub>2</sub> defect passivation and formation in polycrystalline CdTe films by cathodoluminescence, *Phys. Rev. Materials* **5**, 064601 (2021).  
[5] A. Gustafsson and L. Samuelson, Cathodoluminescence imaging of quantum wells: The influence of exciton transfer on the apparent island size, *Phys. Rev. B* **50**, 11827 (1994).  
[6] K. Akiba, N. Yamamoto, V. Grillo, A. Genseki, and Y. Watanabe, Anomalous temperature and excitation power dependence of cathodoluminescence from InAs quantum dots, *Phys. Rev. B* **70**, 165322 (2004).

- [7] M. Merano, S. Sonderegger, A. Crottini, S. Collin, P. Renucci, E. Pelucchi, A. Malko, M. H. Baier, E. Kapon, B. Deveaud, and J.-D. Ganière, Probing carrier dynamics in nanostructures by picosecond cathodoluminescence, *Nature* **438**, 479 (2005).
- [8] M. Kuttge, E. J. R. Vesseur, A. F. Koenderink, H. J. Lezec, H. A. Atwater, F. J. García de Abajo, and A. Polman, Local density of states, spectrum, and far-field interference of surface plasmon polaritons probed by cathodoluminescence, *Phys. Rev. B* **79**, 113405 (2009).
- [9] N. Yamamoto, F. Javier García de Abajo, and V. Myroshnychenko, Interference of surface plasmons and smith-purcell emission probed by angle-resolved cathodoluminescence spectroscopy, *Phys. Rev. B* **91**, 125144 (2015).
- [10] T. Sannomiya, A. Konečná, T. Matsukata, Z. Thollar, T. Okamoto, F. J. García de Abajo, and N. Yamamoto, Cathodoluminescence phase extraction of the coupling between nanoparticles and surface plasmon polaritons, *Nano Lett.* **20**, 592 (2020).
- [11] P. J. Fisher, W. S. Wessels, A. B. Dietz, and F. G. Prendergast, Enhanced biological cathodoluminescence, *Opt. Commun.* **281**, 1901 (2008), optics in Life Sciences.
- [12] K. Nagayama, T. Onuma, R. Ueno, K. Tamehiro, and H. Minoda, Cathodoluminescence and electron-induced fluorescence enhancement of enhanced green fluorescent protein, *The Journal of Physical Chemistry B* **120**, 1169 (2016).
- [13] K. Akiba, K. Tamehiro, K. Matsui, H. Ikegami, and H. Minoda, Cathodoluminescence of green fluorescent protein exhibits the redshifted spectrum and the robustness, *Sci. Rep.* **10**, 17342 (2020).
- [14] L. H. G. Tizei and M. Kociak, Spatially resolved quantum nano-optics of single photons using an electron microscope, *Phys. Rev. Lett.* **110**, 153604 (2013).
- [15] S. Meuret, L. H. G. Tizei, T. Cazimajou, R. Bourrellier, H. C. Chang, F. Treussart, and M. Kociak, Photon bunching in cathodoluminescence, *Phys. Rev. Lett.* **114**, 197401 (2015).
- [16] M. Solà-García, S. Meuret, T. Coenen, and A. Polman, Electron-induced state conversion in diamond NV centers measured with pump-probe cathodoluminescence spectroscopy, *ACS Photonics* **7**, 232 (2020), pMID: 31976357.
- [17] R. Loudon, *The Quantum Theory of Light*, 3rd ed. (Oxford University Press, Oxford, 2000).
- [18] A. Auffèves, D. Gerace, S. Portolan, A. Drezet, and M. F. Santos, Few emitters in a cavity: from cooperative emission to individualization, *New J. Phys.* **13**, 093020 (2011).
- [19] H. A. M. Leymann, A. Foerster, F. Jahnke, J. Wiersig, and C. Gies, Sub- and superradiance in nanolasers, *Phys. Rev. Applied* **4**, 044018 (2015).
- [20] F. Jahnke, C. Gies, M. Afmann, M. Bayer, H. A. M. Leymann, A. Foerster, J. Wiersig, C. Schneider, M. Kamp, and S. Höfling, Giant photon bunching, superradiant pulse emission and excitation trapping in quantum-dot nanolasers, *Nat. Commun.* **7**, 11540 (2016).
- [21] A. Ridolfo, O. Di Stefano, N. Fina, R. Saija, and S. Savasta, Quantum plasmonics with quantum dot-metal nanoparticle molecules: Influence of the fano effect on photon statistics, *Phys. Rev. Lett.* **105**, 263601 (2010).
- [22] D. Zhao, Y. Gu, H. Chen, J. Ren, T. Zhang, and Q. Gong, Quantum statistics control with a plasmonic nanocavity: Multimode-enhanced interferences, *Phys. Rev. A* **92**, 033836 (2015).
- [23] H. A. M. Leymann, C. Hopfmann, F. Albert, A. Foerster, M. Khanbekyan, C. Schneider, S. Höfling, A. Forchel, M. Kamp, J. Wiersig, and S. Reitzenstein, Intensity fluctuations in bimodal micropillar lasers enhanced by quantum-dot gain competition, *Phys. Rev. A* **87**, 053819 (2013).
- [24] C. Redlich, B. Lingnau, S. Holzinger, E. Schlottmann, S. Kreinberg, C. Schneider, M. Kamp, S. Höfling, J. Wolters, S. Reitzenstein, and K. Lüdge, Mode-switching induced super-thermal bunching in quantum-dot microlasers, *New J. Phys.* **18**, 063011 (2016).
- [25] M. Marconi, J. Javaloyes, P. Hamel, F. Raineri, A. Levenson, and A. M. Yacomotti, Far-from-equilibrium route to superthermal light in bimodal nanolasers, *Phys. Rev. X* **8**, 011013 (2018).
- [26] H. A. M. Leymann, D. Vorberg, T. Lettau, C. Hopfmann, C. Schneider, M. Kamp, S. Höfling, R. Ketzmerick, J. Wiersig, S. Reitzenstein, and A. Eckardt, Pump-power-driven mode switching in a microcavity device and its relation to bose-einstein condensation, *Phys. Rev. X* **7**, 021045 (2017).
- [27] M. Schmidt, I. H. Grothe, S. Neumeier, L. Bremer, M. von Helversen, W. Zent, B. Melcher, J. Beyer, C. Schneider, S. Höfling, J. Wiersig, and S. Reitzenstein, Bimodal behavior of microlasers investigated with a two-channel photon-number-resolving transition-edge sensor system, *Phys. Rev. Research* **3**, 013263 (2021).
- [28] S. Meuret, L. H. G. Tizei, T. Auzelle, R. Songmuang, B. Daudin, B. Gayral, and M. Kociak, Lifetime measurements well below the optical diffraction limit, *ACS Photonics* **3**, 1157 (2016).
- [29] H. Lourenço-Martins, M. Kociak, S. Meuret, F. Treussart, Y. H. Lee, X. Y. Ling, H.-C. Chang, and L. H. Galvão Tizei, Probing plasmon-NV<sup>0</sup> coupling at the nanometer scale with photons and fast electrons, *ACS Photonics* **5**, 324 (2018).
- [30] S. Yanagimoto, N. Yamamoto, T. Sannomiya, and K. Akiba, Purcell effect of nitrogen-vacancy centers in nanodiamond coupled to propagating and localized surface plasmons revealed by photon-correlation cathodoluminescence, *Phys. Rev. B* **103**, 205418 (2021).
- [31] S. Meuret, T. Coenen, H. Zeijlemaker, M. Latzel, S. Christiansen, S. Conesa-Boj, and A. Polman, Photon bunching reveals single-electron cathodoluminescence excitation efficiency in InGaN quantum wells, *Phys. Rev. B* **96**, 035308 (2017).
- [32] S. Meuret, T. Coenen, S. Y. Woo, Y.-H. Ra, Z. Mi, and A. Polman, Nanoscale relative emission efficiency mapping using cathodoluminescence  $g^{(2)}$  imaging, *Nano Lett.* **18**, 2288 (2018).
- [33] F. C. van Rijswijk, Photon statistics of characteristic cathodoluminescence radiation: I. theory, *Physica B+C* **82**, 193 (1976).
- [34] F. C. van Rijswijk, Photon statistics of characteristic cathodoluminescence radiation: II. experiment, *Physica B+C* **82**, 205 (1976).
- [35] M. Solà-García, K. W. Mauser, M. Liebrau, T. Coenen, S. Christiansen, S. Meuret, and A. Polman, Photon statistics of incoherent cathodoluminescence with continuous and pulsed electron beams, *ACS Photonics* **8**, 916 (2021).
- [36] M. A. Feldman, E. F. Dumitrescu, D. Bridges, M. F. Chisholm, R. B. Davidson, P. G. Evans, J. A. Hachtel,



- A. Hu, R. C. Pooser, R. F. Haglund, and B. J. Lawrie, Colossal photon bunching in quasiparticle-mediated nanodiamond cathodoluminescence, *Phys. Rev. B* **97**, 081404 (2018).
- [37] V. Gorini, A. Kossakowski, and E. C. G. Sudarshan, Completely positive dynamical semigroups of N-level systems, *J. Math. Phys.* **17**, 821 (1976).
- [38] G. Lindblad, On the generators of quantum dynamical semigroups, *Commun. Math. Phys.* **48**, 119 (1976).
- [39] H.-P. Breuer and F. Petruccione, *The Theory of Open Quantum Systems* (Oxford University Press, Oxford, 2002).
- [40] H. J. Carmichael, *Statistical Methods in Quantum Optics 1: Master Equations and Fokker-Planck Equations* (Springer, Berlin, 1999).
- [41] M. Scully and M. Zubairy, *Quantum Optics* (Cambridge University Press, Cambridge, 1997).
- [42] R. Egerton, *Electron Energy-Loss Spectroscopy in the Electron Microscope* (Springer, New York, 2011).
- [43] L. Mandel and E. Wolf, *Optical Coherence and Quantum Optics* (Cambridge University Press, Cambridge, 1995).
- [44] T. Lettau, H. A. M. Leymann, B. Melcher, and J. Wiersig, Superthermal photon bunching in terms of simple probability distributions, *Phys. Rev. A* **97**, 053835 (2018).
- [45] P. Grünwald, Effective second-order correlation function and single-photon detection, *New J. Phys.* **21**, 093003 (2019).
- [46] V. V. Temnov and U. Woggon, Photon statistics in the cooperative spontaneous emission, *Opt. Express* **17**, 5774 (2009).
- [47] K. Kamide, S. Iwamoto, and Y. Arakawa, Impact of the dark path on quantum dot single photon emitters in small cavities, *Phys. Rev. Lett.* **113**, 143604 (2014).
- [48] R. Loudon, *The Quantum Theory of Light*, 2nd ed. (Clarendon Press, Oxford, 1983).
- [49] J. J. Sakurai and J. Napolitano, *Modern Quantum Mechanics*, 2nd ed. (Addison-Wesley, 2011).